

# Diagnostic Potential of Near-Infrared Raman Spectroscopy for Colon Cancer

Kazuhiro Takabayashi<sup>1)\*</sup> Yoshihisa Saida<sup>1)</sup> Toshiyuki Enomoto<sup>1)</sup>  
Shinya Kusachi<sup>1)</sup> Masahiro Ando<sup>2)</sup> and Hiro-o Hamaguchi<sup>3,4)</sup>

<sup>1)</sup>Division of General and Gastroenterological Surgery (Ohashi), Department of Surgery, School of Medicine, Faculty of Medicine, Toho University

<sup>2)</sup>Consolidated Research Institute for Advanced Science and Medical Care, Waseda University

<sup>3)</sup>Department of Chemistry, School of Science, The University of Tokyo

<sup>4)</sup>Department of Applied Chemistry and Institute of Molecular Science, College of Science, National Chiao Tung University

---

## ABSTRACT

**Background:** Raman spectroscopy measures the specific scattering (“Raman scattering”) of an irradiated target substance illuminated by laser light. The present study used near-infrared Raman spectroscopy to examine spectral differences between specimens of normal and cancerous tissues collected during colon cancer surgery.

**Methods:** Normal and cancerous sites were randomly selected for each specimen, and Raman spectra were obtained using a Raman spectrometer with a 1064 nm excitation fiber optic probe attachment.

**Results:** Although no pronounced marker bands specific to normal or cancerous sites were observed, spectra at normal sites had a higher baseline due to autofluorescence, as compared with cancerous sites. The focus was then changed to the 1003  $\text{cm}^{-1}$  and 1447  $\text{cm}^{-1}$  bands, and the band intensity ratio (1003  $\text{cm}^{-1}$  band intensity)/(1447  $\text{cm}^{-1}$  band intensity) was calculated for all spectra. The 1657  $\text{cm}^{-1}$  band was also examined, and the band intensity ratio (1657  $\text{cm}^{-1}$  band intensity)/(1447  $\text{cm}^{-1}$  band intensity) was calculated. Using the two types of band intensity ratios, we obtained a two-dimensional plot, which made it possible to differentiate normal and cancerous sites with 91 % sensitivity and 91 % specificity.

**Conclusions:** If the present method becomes applicable endoscopically, it will enable easy collection of Raman spectra of colon cancer biopsy samples. Thus, analysis of tissues based on information regarding their molecular structure is now feasible.

Toho J Med 1 (3): 35–40, 2015

---

**KEYWORDS:** Raman spectroscopy, colon cancer, autofluorescence, band intensity ratio

Raman spectroscopy measures the specific scattering (“Raman scattering”) produced by an irradiated target

substance that is illuminated by laser light. The spectrum that represents this scattering (Raman spectrum) is called

---

1) 2–17–6 Ohashi, Meguro, Tokyo 153–8515

2) 513 Wasedatsurumakicho, Shinjuku, Tokyo 162–0041

3) 7–3–1 Hongo, Bunkyo, Tokyo 113–0033

4) 1001 Ta Hsueh Road Hsinchu 30010, Taiwan

\*Corresponding Author: tel: 03 (3468) 1251

e-mail: takaba8shi@yahoo.co.jp

Received Jan. 19, 2015; Accepted June 29, 2015

Toho Journal of Medicine 1 (3), Sept. 1, 2015.

ISSN 2189–1990, CODEN: TJMOA2

the “fingerprint” of a molecule and has patterns that differ depending on the molecular structure or composition of the tissue.<sup>1)</sup> Because detailed information on molecular structure can be acquired without preprocessing, research aiming to use this method in various medical applications has been progressing. When this spectroscopic method is used in clinical diagnosis, it is likely to lead to fast and objective diagnosis through quantification of information on molecular structure obtained from Raman spectra.

The present study used near-infrared Raman spectroscopy to capture differences in spectra between normal and cancer sites from biopsy samples collected during colon cancer surgery, with the aim of eventually using this technique for colon cancer diagnosis.

### Participants and Methods

The present study analyzed specimens collected during surgery. The median age of the 55 patients (30 men) was 77 years. The histologic types of the colon cancers were well-differentiated adenocarcinoma ( $n=18$ ), moderately differentiated adenocarcinoma ( $n=31$ ), poorly differentiated adenocarcinoma ( $n=2$ ), and mucinous adenocarcinoma ( $n=4$ ). There were 10 stage I patients, 25 stage II patients, 11 stage IIIa patients, 7 stage IIIb patients, and 2 stage IV patients.

A Raman spectrometer with a 1064 nm excitation fiber optic probe attachment was used for the measurements (Fig. 1). The probe (InPhotonics Inc., Norwood, MA, USA) comprised a 100  $\mu\text{m}$  excitation fiber and a 300  $\mu\text{m}$  collection fiber. A sapphire ball lens (focal length 1 mm) attached to the end of the probe was used for laser irradiation and

collection of Raman-scattered light. The diameter of the probe was 9 mm and the spot size of laser irradiation was approximately 100  $\mu\text{m}$ . By using an apparatus with a fiber optic probe, it was possible to easily select the measurement position or site on the sample tissue and thus obtain a Raman spectrum. The intensity of excitation light at the sample position was 40 mW, and it required 1 min of exposure to obtain 1 spectrum. To avoid the effects of blood, the specimen surfaces were wiped to remove blood. No further processing was done, and measurements were performed within 1 h after surgical removal of the tissue.

At the time of measurement, normal and cancerous tissue sites for measurement were randomly selected within the specimen, after which Raman spectra were obtained. The measurement site of the normal tissue was sufficiently far from the cancerous site ( $\geq 1$  cm apart) and was chosen from a region that was considered clearly normal. Raman spectra were obtained from 181 cancerous and 157 normal tissue sites from 55 specimens.

The Mann-Whitney  $U$  test was used for all statistical analyses, and a  $p$  value less than 0.05 was considered to indicate statistical significance.

We obtained approval from the ethics committee at Toho University Ohashi Medical Center (approval no. 22-67), and informed consent was obtained in advance from patients who participated in this study.

The authors have no potential conflict of interest to disclose.

### Results

Fig. 2a shows the mean Raman spectra for normal and

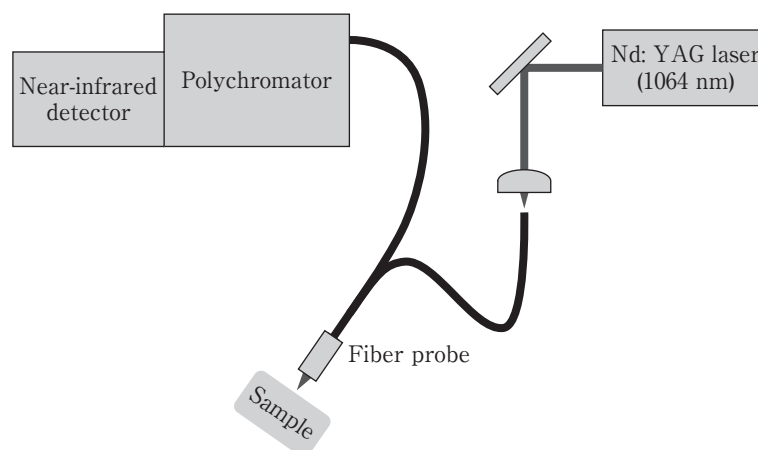


Fig. 1 Schematic diagram of a Raman spectrometer with a 1064 nm excitation fiber optic probe attachment, as used in the present study. Nd: YAG (neodymium-doped yttrium aluminum garnet)

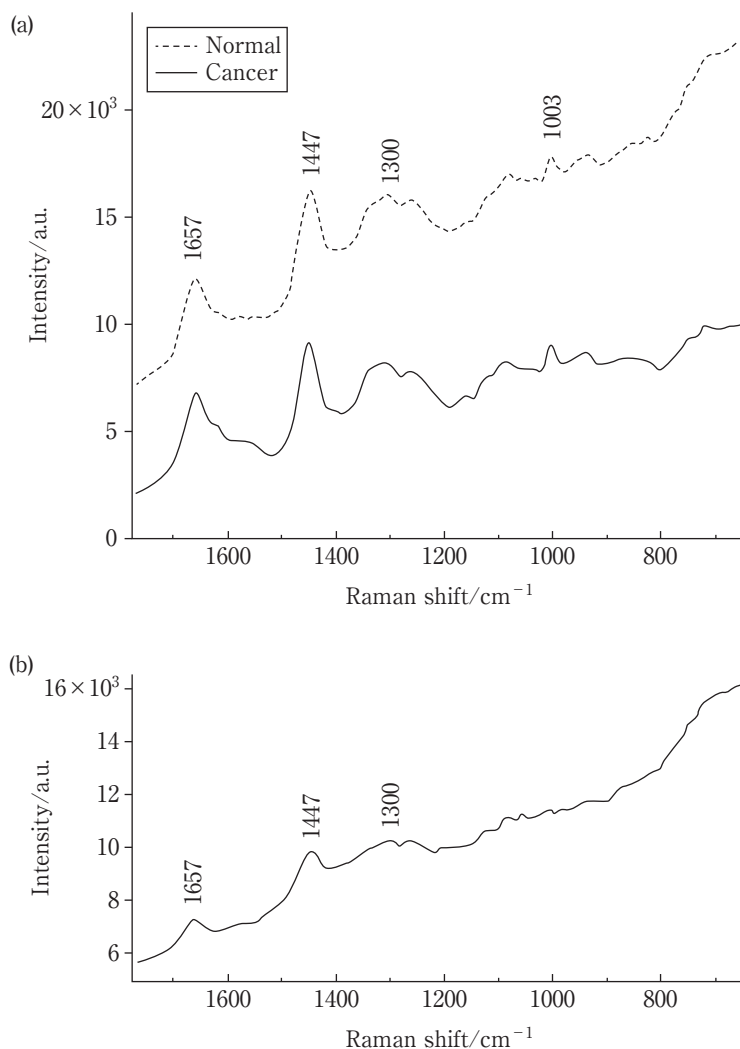


Fig. 2 (a) The mean Raman spectra of normal and cancerous tissue sites obtained from 55 specimens. (b) The difference spectrum, in which the cancerous site spectrum is subtracted from the normal site spectrum. The spectrum is normalized to the band intensity at  $1003\text{ cm}^{-1}$ , which is assigned to the phenylalanine residue of protein.

cancerous tissue sites obtained in measurements of the 55 specimens. To detect more-detailed differences between each of the Raman spectra, a difference spectrum was obtained by subtracting the cancerous site spectrum from the normal site spectrum. Fig. 2b shows the difference spectrum after normalizing to band intensity at  $1003\text{ cm}^{-1}$ , which corresponds to the phenylalanine residue of protein. The obtained spectrum shows marked Raman bands at  $1300$ ,  $1447$ , and  $1657\text{ cm}^{-1}$ , which are considered to belong to lipids. These results suggest that the abundance ratio of protein and lipids differ between normal sites and cancerous sites. In other words, the protein-to-lipid ratio is higher for cancerous sites than for normal sites. The normal tis-

sue spectrum showed an increase in the overall baseline, as compared with the cancerous site spectrum, an effect likely due to autofluorescence from the samples. Thus, the baseline height was set at the  $1447\text{ cm}^{-1}$  band, which corresponds to the CH bending vibrations of lipids and protein, as the fluorescence intensity, and this was compared between normal and cancerous sites. To correct for measurement differences caused by measurement conditions such as intensity of excitation light, the spectra were normalized to the baseline height at the  $1447\text{ cm}^{-1}$  band intensity, and autofluorescence intensity was quantitatively compared.

Fig. 3 shows the frequency distribution of the autofluo-

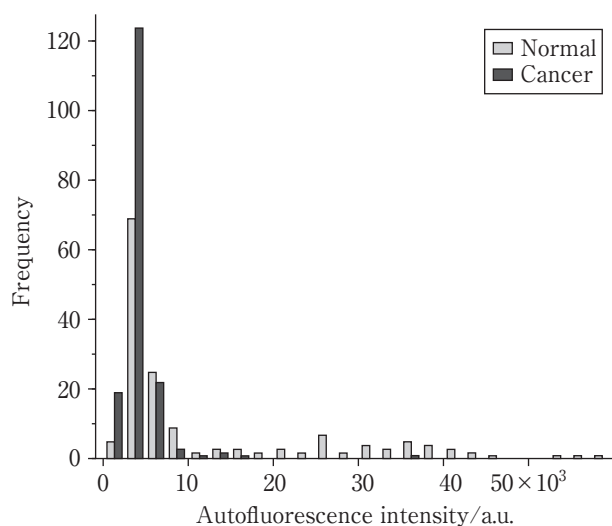


Fig. 3 Frequency distribution of autofluorescence intensity calculated from all spectra of normal and cancerous sites. As compared with cancerous sites, normal sites were more likely to exhibit greater autofluorescence intensity.

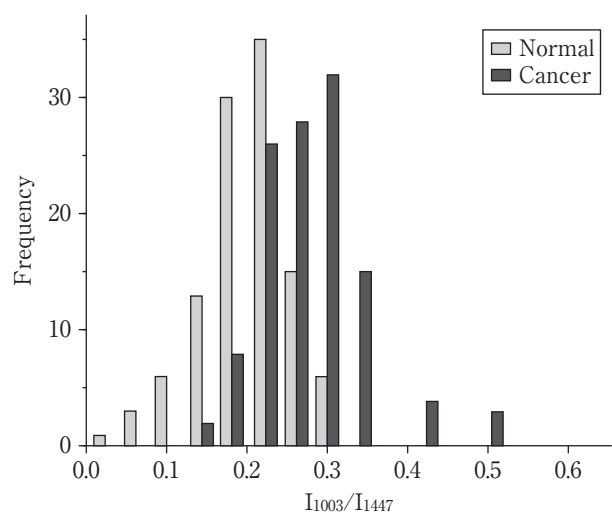


Fig. 4 Frequency distribution of the band intensity ratio for all spectra, calculated from the 1003  $\text{cm}^{-1}$  band, which belongs to protein only, and the 1447  $\text{cm}^{-1}$  band, which belongs to both proteins and lipids.

rescence intensities that were calculated in all spectra of normal and cancerous sites. As compared with cancerous sites, there was a significantly higher incidence of high autofluorescence intensities in normal sites ( $p < 0.001$ ). Thus, it might be possible to use fluorescence intensities to differentiate normal and cancerous sites. In contrast, there were no distinct marker bands that were specific to normal or cancerous sites, and Raman bands were detected at 1003, 1447, and 1657  $\text{cm}^{-1}$  in both spectra. These bands are

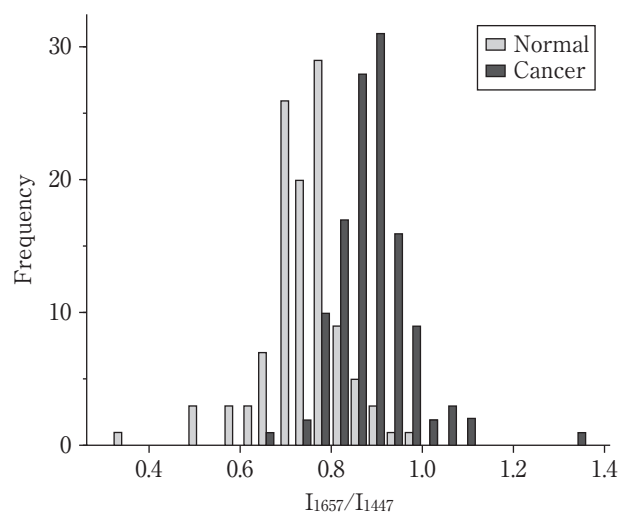


Fig. 5 The intensity ratio of the 1657  $\text{cm}^{-1}$  band (corresponding to C=C stretching vibration of lipids and to the protein amide I mode) to the 1447  $\text{cm}^{-1}$  band was calculated. There was a significant difference in the distributions between the two types of tissues.

assigned to the ring-breathing vibration of the phenylalanine residue of protein, CH bending vibrations of protein and lipids, the superposition of protein amide I mode, and C=C stretching vibrations of lipids, respectively.

Therefore, we evaluated the 1003  $\text{cm}^{-1}$  band assigned to protein only, and the 1447  $\text{cm}^{-1}$  band assigned to both protein and lipids, and band intensity ratios, *i.e.*, (1003  $\text{cm}^{-1}$  band intensity)/(1447  $\text{cm}^{-1}$  band intensity), were calculated in all spectra acquired in this study. The frequency distribution of this intensity ratio is shown in Fig. 4 and significantly differs between normal and cancerous sites ( $p < 0.001$ ).

Similarly, the 1657  $\text{cm}^{-1}$  band belonging to the protein amide I mode and the C=C stretching vibration of lipids was examined, and the band intensity ratio—(1657  $\text{cm}^{-1}$  band intensity)/(1447  $\text{cm}^{-1}$  band intensity)—was calculated. The distribution of this intensity ratio, as shown in Fig. 5, also significantly differed between the 2 tissue sites ( $p < 0.001$ ). Fig. 6 shows a 2-dimensional plot obtained using the above 2 types of band intensity ratios.

Use of these 2 indices made it possible to more clearly differentiate normal and cancerous sites. In addition, by determining the cutoff point based on the receiver operating characteristic (ROC) curve, and distinguishing normal and cancerous sites with a straight line, as shown in Fig. 7, it was possible to obtain 91% sensitivity and 91% specificity with our measurement results.

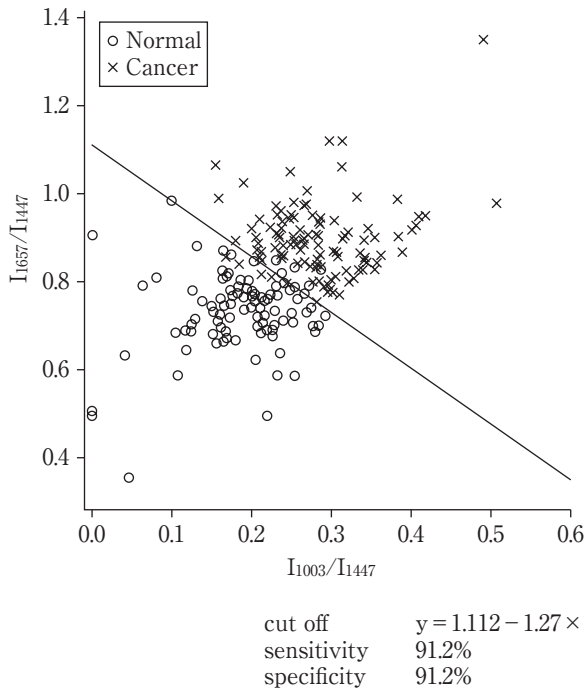


Fig. 6 A two-dimensional plot was created from the two types of band intensity ratios obtained in this study. The cutoff point is determined based on the ROC curve, and normal and cancerous sites can be discriminated by using a straight line.

ROC: receiver operating characteristic

## Discussion

Recent years have seen remarkable advances in endoscopic diagnosis of colon cancer. These methods include pit pattern classification using crystal violet staining, narrow band imaging (NBI), and image enhancement and magnified observation using flexible spectral imaging (FICE). However, it is not feasible to endoscopically distinguish between malignant and normal tissue or to differentiate advanced cancer from early cancer.<sup>2)</sup> These methods primarily involve detailed observations of the mucosal surface or submucosal blood vessels. Thus, there is a limitation in their capabilities to assess submucosal infiltration distance, which is the branching point between endoscopic treatment and surgical treatment. To overcome this limitation, a new technique must be developed to evaluate and diagnose the molecular structure of the layer several millimeters below the mucosa.

For this reason, we selected Raman spectroscopy, which is widely used in industrial measurements. When scattered light from an irradiated substance is analyzed, there is a mixture of light with wavelengths that are different

from the incident light. This is caused by the energy transfer from the interaction between light and target substance and is called the Raman effect, after the Indian physicist Chandrasekhara Raman, who discovered the phenomenon.

Raman spectroscopy uses this Raman scattering and, as described above, observes the specific scattering produced by an irradiated target material illuminated by laser light.<sup>1)</sup> The Raman spectrum contains information that is unique to a specific substance, and because the Raman spectra peaks of functional groups that characterize a substance are known, it is possible to infer the partial structure of the substance or compound. With Raman spectroscopy, detailed molecular structures can be obtained quickly without preprocessing or damaging the tissue.<sup>3)</sup> Previous attempts to use this technology utilized an excitation light around 800 nm for clinical diagnosis of colon cancer<sup>3-9)</sup>; however, the Raman scattering intensity is extremely weak, and measurements were complicated by fluorescence noise produced from living tissue at the time of laser illumination.

To measure Raman scattering, it is necessary to illuminate the target sample with excitation laser light. However, if the sample or minute contaminants in the sample absorb the excitation laser light and emit this energy as fluorescence, its intensity becomes greater than the Raman scattering intensity, by several orders of magnitude, which completely masks the weak Raman spectrum. Near-infrared excitation Raman spectroscopy with an neodymium-doped yttrium aluminum garnet (Nd:YAG) laser at a fundamental wavelength of 1064 nm was used in the present study<sup>10)</sup> and enabled high S/N Raman spectra, by avoiding fluorescence interference from biological tissue. This made it possible to obtain measurements with minimal noise. This method enabled collection of information on molecular scientific and numeric analysis.

Abundance ratios of molecules such as protein, lipids, and nucleic acids differ between cancerous sites and normal sites. Previous studies of lung tissue showed that Raman spectra are vastly different between normal and cancerous sites and that the vibration intensity of the protein main chain called the amide I band (at  $1659 \text{ cm}^{-1}$ ) increases dramatically with oncogenesis.<sup>11,12)</sup> In the present study, there were no pronounced marker bands, but normal and cancerous sites could be distinguished by differences in fluorescence intensities. In addition, when normal and cancerous sites were distinguished at the cutoff point with a

straight line, as shown in Fig. 7, the measurement results had 91% sensitivity and 91% specificity.

The present study compared cancerous and non-cancerous sites; however, in the future, along with evaluation of histopathologic results, it will be necessary to focus on lesions with unclear malignancy status, or on early cancer (especially submucosal cancer), to determine whether the degree of submucosal infiltration causes a change in the spectrum. The laser used for Raman excitation can be illuminated from a fiber optic probe; the device can therefore be inserted from the opening of endoscope forceps. This enables endoscopic, non-contact, and *in vivo* colon cancer diagnosis. Moreover, we anticipate that some biopsies and polypectomies that are currently performed to determine whether a lesion is benign or malignant will become unnecessary, thus potentially reducing physical burdens on patients and economic burdens on national health care systems. Furthermore, if it becomes possible to determine the degree of submucosal infiltration at an early cancer stage, clinicians will be able to obtain useful information in determining whether endoscopic resection is necessary.

### Conclusion

Raman spectra of colon cancer biopsy samples were easily obtained using 1064 nm excitation near-infrared Raman spectroscopy. Thus, it is now feasible to analyze tissues on the basis of information on molecular structure.

### References

1) Hamaguchi H, Hirakawa A. Raman Bunkoho [Raman Spectros-

- copy]. Gakkai Shuppan Center, Tokyo, 1988. Japanese.
- 2) Okamoto Y, Kimura R, Igarashi Y, Tagata T, Mitsunaga A, Yamaguchi T, et al. [A review of the pathological issues of endoscopic resection for early colorectal carcinomas]. *Nihon Daicho Komon Byo Gakkai Zasshi*. 2012; 65: 808-14. Japanese.
  - 3) Chowdary MV, Kumar KK, Thakur K, Anand A, Kurien J, Krishna CM, et al. Discrimination of normal and malignant mucosal tissues of the colon by Raman spectroscopy. *Photomed Laser Surg*. 2007; 25: 269-74.
  - 4) Misra SP, Dwivedi M, Sharma K. Colon tumors and colonoscopy. *Endoscopy*. 2011; 43: 985-9.
  - 5) Molckovsky A, Song LM, Shim MG, Marcon NE, Wilson BC. Diagnostic potential of near-infrared Raman spectroscopy in the colon: differentiating adenomatous from hyperplastic polyps. *Gastrointest Endosc*. 2003; 57: 396-402.
  - 6) Short MA, Lam SF, Owen DA, Macaulay C, Tai IT, Zeng H. Development of an endoscopic Raman spectroscopy system for the improving detection of early colonic neoplasias [abstract]. *Gastrointest Endosc*. 2011; 73(4 Suppl): AB371-2.
  - 7) Andrade PO, Bitar RA, Yassoyama K, Martinho H, Santo AME, Bruno PM, et al. Study of normal colorectal tissue by FT-Raman spectroscopy. *Anal Bioanal Chem*. 2007; 387: 1643-8.
  - 8) Shim MG, Song LM, Macron NE, Wilson BC. *In vivo* near-infrared Raman spectroscopy: demonstration of feasibility during clinical gastrointestinal endoscopy. *Photochem Photobiol*. 2000; 72: 146-50.
  - 9) Wood JJ, Kendall C, Hutchings J, Lloyd GR, Stone N, Shepherd N, et al. Evaluation of a confocal Raman probe for pathological diagnosis during colonoscopy. *Colorectal Dis*. 2014; 16: 732-8.
  - 10) Min YK, Ito T, Hamaguchi H. [Near-infrared spectroscopy: V. near-infrared excited Raman spectroscopy]. *Bunko Kenkyu*. 2004; 53: 318-31. Japanese.
  - 11) Yamazaki H, Kaminaka S, Kohda E, Mukai M, Hamaguchi HO. The diagnosis of lung cancer using 1064-nm excited near-infrared multichannel Raman spectroscopy. *Radiat Med*. 2003; 21: 1-6.
  - 12) Min YK, Yamamoto T, Kohda E, Ito T, Hamaguchi H. 1064 nm near-infrared multichannel Raman spectroscopy for fresh human lung tissues. *J Raman Spectrosc*. 2005; 36: 73-6.